Identification of diffusion weighted imaging would be affected before and after Gd-EOB-DTPA in patients with focal hepatic lesions: an observational study

Hehan Tang[1#^], Yuan Yuan[1#], Liping Deng[1], Yi Wei[1], Guoyong Chen[1], Tong Zhang[1], Lisha Nie[2], Xiaocheng Wei[2], Bin Song[1], Zhenlin Li[1]

[1]Department of Radiology, West China Hospital, Sichuan University, Chengdu, China; [2]GE Healthcare China, Beijing, China

Contributions: (I) Conception and design: Z Li, B Song; (II) Administrative support: Z Li, B Song; (III) Provision of study materials or patients: H Tang, Y Yuan, L Deng, G Chen; (IV) Collection and assembly of data: H Tang, T Zhang, Y Wei; (V) Data analysis and interpretation: Y Wei, L Nie, X Wei; (VI) Manuscript writing: All authors; (VII) Final approval of manuscript: All authors.

[#]These authors contributed equally to this work.

Correspondence to: Zhenlin Li, PhD; Bin Song, MD. Department of Radiology, West China Hospital, Sichuan University, No. 37, Guoxue Alley, Chengdu 610041, China. Email: lzlcd0l@126.com; songlab_radiology@163.com.

Background: Inserting diffusion weighted imaging (DWI) into the time interval between post contrast and hepatobiliary phase (HBP) is time saving and health economic friendly. However, whether DWI would be affected before and after Gd-EOB-DTPA is still unknown. This study aims to validate whether the DWI at both low and high b-values is affected before and after Gd-EOB-DTPA enhancement.

Methods: From July 2019 to November 2019, seventy-three patients who satisfied the inclusion criteria were enrolled. Those patients were scanned with multiple b-value (b-value of 0, 50, 800, 1,000, and 1,200 s/mm^2) DWI using a 3.0 T magnetic resonance (MR) scanner before and after the injection of Gd-EOB-DTPA. The final imaging diagnosis of the malignant liver lesions were made by histopathological analysis. The lesion-liver contrast intensity ratio (CIR) and the apparent diffusion coefficients (ADCs) of hepatic parenchyma and lesions at each b-value was evaluated. The Student's *t*-test or Mann-Whitney U test was used to compare the CIR and ADC between the MR images before and after contrast agent injection. In addition, the Student's *t*-test or Mann-Whitney U test was used to compare the ADC values between benign and malignant lesions. Receiver operating characteristics (ROC) curves were used to assess the area under the curve (AUC) of the ADC values in differentiating between benign and malignant lesions.

Results: For the CIRs comparison, the CIRs showed no statistical significance before and after Gd-EOB-DTPA on b =0 (1.34±1.15 *vs.* 1.45±1.48, P=0.664), b=50 (1.23±1.13 *vs.* 1.35±1.34, P=0.982), b=800 (1.19±0.87 *vs.* 1.19±0.94, P=0.946), b=1,000 (1.21±0.90 *vs.* 1.32±1.05, P=0.294) and b=1,200 (1.25±1.03 *vs.* 1.45±1.48, P=0.165) s/mm^2. For the ADC value comparison, the ADC also showed no statistical significance before and after Gd-EOB-DTPA on b=50 (4.04±2.82 *vs.* 3.91±3.00, P=0.151), b=800 (1.68±0.71 *vs.*1.67±0.76, P=0.163), b=1,000 (1.53±0.69 *vs.*1.50±0.70, P=0.078) and b=1,200 (1.48±0.66 *vs.* 1.48±0.70, P=0.294) s/mm^2.

Conclusions: DWI scanned between the interval of dynamic enhanced imaging and HBP imaging can save overall scanning time without influencing the CIRs, ADCs, and diagnostic capabilities of hepatic lesions at both low and high b-values.

Keywords: Diffusion weighted imaging (DWI); Gd-EOB-DTPA; b-value; hepatic lesion

Submitted Jan 27, 2022. Accepted for publication Mar 21, 2022.

doi: 10.21037/atm-22-962

View this article at: https://dx.doi.org/10.21037/atm-22-962

^ ORCID: 0000-0002-3882-4270.

© Annals of Translational Medicine. All rights reserved.

Introduction

Liver cancer is the fifth most common cancer and the second most frequent cause of cancer-related deaths in men worldwide (1,2). Accurate tumor detection and early identification diagnosis is valuable in the treatment of liver cancer patients (3). At present, Gd-EOB-DTPA has been widely used in liver magnetic resonance imaging (MRI) due to its characterization of intra and extracellular ability, which enables not only traditional arterial phase imaging of hepatic lesions but also further provides the specific hepatobiliary phase (HBP). However, despite the considerable advantages of Gd-EOB-DTPA MRI, its major problem is the fact that the HBP can only be obtained after approximately a 20-minute delay following the contrast agent injection, and if no sequences are scanned during the interval between dynamic scans and HBP, the patient throughput will be directly influenced.

Several strategies have been used to overcome this problem, including shortening the delay time of the HBP (4) and optimizing the scanning of the magnetic resonance (MR) protocol (5-9). Of these, the adjustment of the diffusion weighted imaging (DWI) sequence scanning order from pre-contrast to post-contrast is feasible and crucial. As an advanced MR technique, DWI can effectively detect and differentiate liver lesions, and has been widely used in clinical practice (10). However, it is often based on the single-shot-fast-spin-echo with echo-planner-imaging (SSFSE-EPI) sequence, which requires increasing the number of excitations (NEX) to improve the signal-to-noise ratio (SNR), especially in DWI with a high b-value. Meanwhile, the respiratory trigger (RT) is often used in liver DWI to remove the impact of respiratory motion, which will further extend the acquisition time. Due to the above reasons, DWI of the liver typically takes around 5 minutes in a clinical scanning setting. Some previous research has proposed that adjustment of the DWI scanning order can both meet the clinical diagnosis needs and save the overall acquisition time of liver MRI with Gd-EOB-DTPA. Muhi *et al.* (6) found that T2-weighted imaging (T2WI) and DWI with Gd-EOB-DTPA are feasible for diagnosis and do not compromise the apparent diffusion coefficient (ADC) of focal hepatic lesions. Choi *et al.* (7) also reported that the acquisition of DWI during the interval between dynamic MRI and hepatobiliary imaging can be effective and time-saving, without compromising the contrast-to-noise ratio (CNR) and ADC values of focal hepatic lesions. However, most of these reports only explored the fitting ADC values of both low and high b-valve DWI, and few studies have investigated whether ADC values is affected at both low and high b-values. To our knowledge, no studies have been investigated to directly comparison the DWI at both low and high b-values would be affected before and after Gd-EOB-DTPA enhancement about the image quality and diagnostic performance.

Therefore, the purpose of this paper was to validate whether DWI at both low and high b-values is affected before and after Gd-EOB-DTPA enhancement. We present the following article in accordance with the STARD reporting checklist (available at https://atm.amegroups.com/article/view/10.21037/atm-22-962/rc).

Methods

Patients

The protocol was registered at Chinese Clinical Trial Registry (clinical trial registration No. ChiCTR1900026668). The study was conducted in accordance with the Declaration of Helsinki (as revised in 2013). This diagnostic and observational study was approved by the institutional review board of biomedical ethics branch of West China Hospital, Sichuan University [No. 2016(297)], and written informed consent was obtained from all patients. The sample size was considered according to the clinical experience and the inclusion of 60 patients may satisfy the requirements. From July to November 2019, 87 consecutive patients (including 59 men and 28 women; age range, 21–82 years; mean age: 50.71 years) who were suspected of having focal hepatic lesions underwent with gadoxetic acid-enhanced liver MRI were prospectively included. The inclusion criteria were as follows: (I) patients with no MR examination contraindications; (II) those with no history of local liver treatment; and (III) lesions with diameter ≥1 cm. Additionally, patients were excluded for the following reasons: (I) lesions located in the left lateral lobe below the heart (n=2) or at the edge of the liver (n=3); (II) those with uneven breathing, resulting in severe motion artifact interference (n=5); and (III) patients that could not tolerant the MR examination (n=4). Finally, 73 patients with 92 focal hepatic lesions were included (*Figure 1*), and the final diagnosis of these lesions were made by histopathological analysis (malignant lesions) or long-time follow up (benign lesions).

MRI protocols

MRI was carried out by using a 3.0 T MR system (Discovery

© Annals of Translational Medicine. All rights reserved.

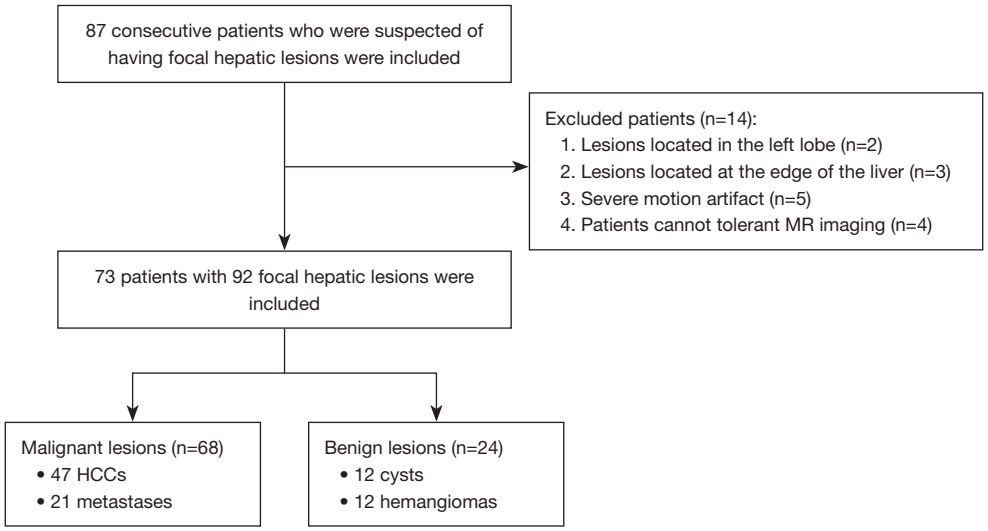

Figure 1 Flow chart of the study population selection. MR, magnetic resonance; HCCs, hepatocellular carcinomas.

Table 1 MRI parameters of the routine MR sequences

Parameters	Tra-T1WI IP/OP	Dyn-T1WI	Ax T2WI-FS	DWI	3D T1WI in HBP
Repetition time (ms)	150	6	2–3 respiratory cycle	1–2 respiratory cycle	6.1
Echo time (ms)	2.3/5.8	1.4	69.4	70	1.4
Field of view (cm^2)	40×40	38×30.4	40×40	40×40	38×30.4
Matrix	288×192	300×204	320×320	128×128	300×204
Slice thickness (mm)	6	4	6	6	3
Acceleration factor	2	2	2	2	2
Resolution (mm^2)	1.39×2.08	1.27×1.49	1.25×1.25	3.125×3.125	1.27×1.49

MRI, magnetic resonance imaging; MR, magnetic resonance; Tra, transverse; T1WI, T1-weighted imaging; IP/OP, in-phase/out-phase; Dyn, dynamic; Ax, axial; T2WI, T2-weighted imaging; FS, fat-suppressed; DWI, diffusion weighted imaging; 3D, three-dimensional; HBP, hepatobiliary phase.

MR 750w, GE Healthcare, Milwaukee, USA). A 16-channel phased-array torsor coil (GE Medical System) was used for all examinations. Routine liver MRI protocols, including T1-weighted imaging (T1WI) using in-phase and out-of-phase spoiled gradient echo (SPGR), dynamic T1WI using three-dimensional (3D) liver imaging with volume acceleration-flexible (LAVA-FLEX), T2WI using fast spin echo (FSE) with PROPELLER technique and chemical-shift fat saturation, SSFSE-EPI DWI with RT and multi-b-value (b=0, 50, 800, 1,000, and 1,200 s/mm^2), and 3D T1WI LAVA-FLEX in HBP, were performed before and after injecting gadoxetic acid. The arterial phase images were acquired in a 17 s long breath hold with a 20 s delay following injection of the gadoxetate acid disodium (Primovist, Bayer Pharma AG, Berlin, Germany) at an injection rate of 1 mL/s. The mean delay time for the portal venous phase, delayed phase, and HBP were 60 s, 180 s, and 20 min, respectively. Detailed information of the MR parameters is listed in *Table 1*.

Imaging analysis

Two abdominal radiologists (with 30 and 9 years in the interpretation of liver MRI, respectively) who were blinded to all patient information reviewed the MR images. For the signal intensity (SI) of normal liver parenchymal measurement, the regions of interest (ROIs) were placed in the posterior right hepatic lobe, specifically at the level of the main portal vein and its right branches, while excluding vessels and artifacts. In addition, for the SI of lesion

© Annals of Translational Medicine. All rights reserved.

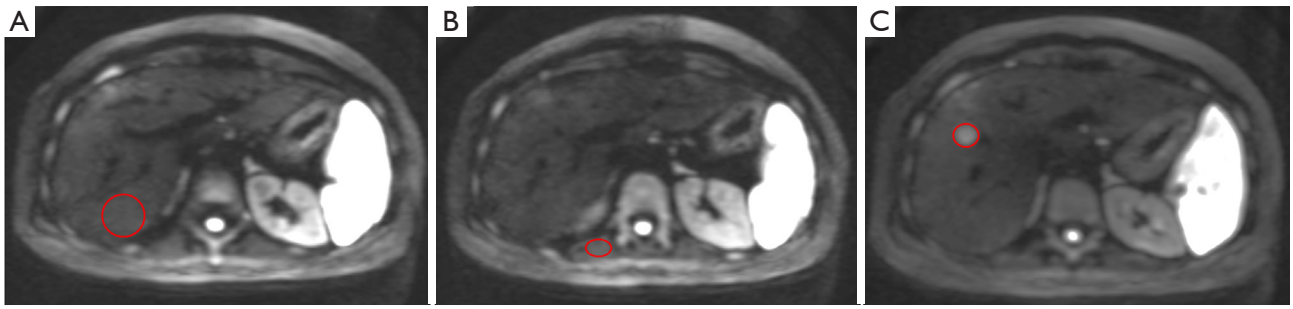

Figure 2 The drawing methods of ROIs. (A) The circle indicates the ROI of normal hepatic parenchyma; (B) the oval circle indicates the ROI of skeletal muscle; (C) the oval circle indicates the ROI of the lesion. ROIs, regions of interest.

measurement, the ROIs were positioned in the homogeneous areas, while avoiding artifacts and major vascular structures, as well as necrosis and hemorrhage of the lesions. The SI of the skeletal muscle in the same section were also recorded (*Figure 2*). The ROIs were manually and carefully positioned to ensure identical location among different b-values of the DW images (11). The contrast intensity ratio (CIR) of lesions at each b-value image before and after contrast agent injection was calculated using the following equation (6):

$$CIR = \frac{\left[SI_{(lesion)} - SI_{(liver)}\right]}{SI_{(muscle)}} \quad [1]$$

Furthermore, four different ADC values of the normal liver parenchyma and lesions were also measured, including $ADC_{(50)}$ (calculated by b=0, 50 s/mm^2), $ADC_{(800)}$ (calculated by b=0, 800 s/mm^2), $ADC_{(1000)}$ (calculated by b=0, 1,000 s/mm^2), and $ADC_{(1200)}$ (calculated by b=0, 1,200 s/mm^2).

Statistical analysis

Continuous variables were firstly checked for normality using the Kolmogorov-Smirnov test, and the Student's *t*-test or Mann-Whitney U test were used to compare the CIRs and ADCs between the MR images before and after contrast agent injection. In addition, the Student's *t*-test or Mann-Whitney U test were also used to compare the ADC values between benign and malignant lesions. Receiver operating characteristics (ROC) curves were drawn to assess the area under the curve (AUC) of the ADC values to differentiate between benign and malignant lesions, as well as their 95% confidence interval (CI). The diagnostic sensitivity and specificity were also calculated. A P value less than 0.05 was considered to be statistical significance. All statistical analyses were performed by using the SPSS 23.0 statistical software package (SPSS Inc., Chicago, IL, USA).

Results

Patients' characteristics

In total, 73 patients (age: 51.64±10.59 years), including 50 males (age: 51.30±10.10 years) and 23 females (age: 52.39±11.55 years), with 92 focal hepatic lesions were included. Of these, there were 68 malignant lesions [47 hepatocellular carcinomas (HCCs) in 44 patients and 21 metastases in 15 patients] and 24 benign lesions (12 cysts in 10 patients and 12 hemangiomas in 11 patients). Patients with liver metastases were mainly caused by the following primary tumors: breast cancer (n=3), colorectal carcinoma (n=7), gastric carcinoma (n=1), renal cell carcinoma (n=1), gallbladder carcinoma (n=1), esophageal carcinoma (n=1), and melanoma (n=1).

Comparison of CIRs

For the CIRs measurement of all lesions, the CIRs value of the b=0 (P=0.664; Z=−0.435), 50 (P=0.982; Z=−0.023), 800 (P=0.946; Z=−0.068), 1,000 (P=0.294; Z=−1.050), and 1,200 (P=0.165; Z=−1.389) s/mm^2 on the unenhanced DW images were not significantly compared with each b-value on the enhanced MR images (*Figure 3*). In addition, for the CIRs measurement of various lesions, no difference was observed between the unenhanced and enhanced MR images (all P>0.05). Detailed information about the CIRs of focal hepatic lesions on unenhanced and enhanced DW images are shown in *Table 2*.

Comparison of ADCs

For the ADC measurement of all lesions, the ADC values of the b=50 (P=0.151; Z=−1.431), 800 (P=0.163; Z=−1.394), 1,000 (P=0.078; Z=−1.765), and 1,200 (P=0.294;

© Annals of Translational Medicine. All rights reserved.

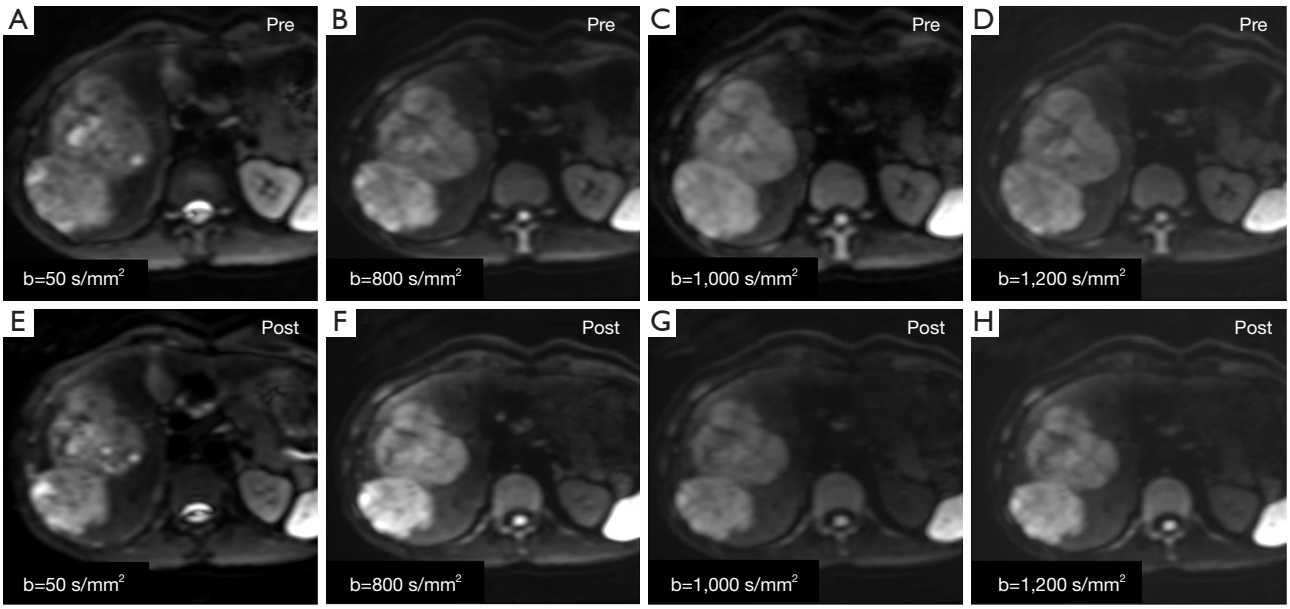

Figure 3 Male, 24 years old, surgically confirmed HCC in the right liver lobe. (A-D) DWI pre-contrast; (E-H) DWI post-contrast. (A,E) b-value =50 s/mm^2; (B,F) b-value =800 s/mm^2; (C,G) b-value =1,000 s/mm^2; (D,H) b-value =1,200 s/mm^2. The lesion displays in enhanced DWI were not different from those of unenhanced DWI. HCC, hepatocellular carcinoma; DWI, diffusion weighted imaging.

Z=–1.049) s/mm^2 on the unenhanced DW images were not significantly different compared with each b-value on the enhanced MR images (*Figure 4*). A decreasing tendency for ADCs with focal hepatic lesions on both pre-contrast and post-contrast DWI images was observed with increased b-values. *Table 3* shows the analysis results of ADCs between pre-contrast and post-contrast DWIs.

Diagnostic performance evaluation

When the b-value was 800, 1,000, and 1,200 s/mm^2, the ADC values of benign lesions were statistically higher than those of malignant tumors on both unenhanced and enhanced images (all P<0.01). However, for the b-value =50 s/mm^2, no statistical difference was observed between the ADCs in malignant and benign tumors [$P_{(pre)}$ =0.606; $P_{(post)}$ =0.637]. Additionally, for enhanced images, the b-value =1,200 s/mm^2 had the largest AUC value of 0.889(95% CI: 0.807–0.971), followed by b-value =1,000 (AUC =0.868 s/mm^2; 95% CI: 0.784–0.952). For qualitative diagnosis, no statistical difference was observed in these b-values in differentiating between benign and malignant lesions, and the diagnostic performance for both before and after Gd-EOB-DTPA were 100% for sensitivity, and 100% for specificity.

Discussion

In the present study, we compared the CIRs and ADCs of various types of hepatic lesions between before and after Gd-EOB-DTPA injection on DWI with multiple b-values (b=0, 50, 800, 1,000 and 1,200 s/mm^2), and our results showed that there were no statistically significant differences in the CIRs and ADCs between the DW images before and after contrast agent injection. Previous studies have reported that when the b-value was less than 100–150 s/mm^2, the intra-hepatic vascular signal would be lost, producing a so-called black blood image, which improved the detection of focal liver lesions (12,13), and a higher b-value (b-value ≥500 s/mm^2) could provide diffusion information that helps to characterize focal liver lesions (14). Thus, when performing a DWI scan on the liver, using both lower and higher b-values (e.g., b-value ≤100 s/mm^2, and ≥500 s/mm^2) was recommended for imaging (15). In this study, the DWI sequence included one low b-value (50 s/mm^2) and three high b-values (800, 1,000, 1,200 s/mm^2), and the effect of the Gd-EOB-DTPA on the DW images and ADC value of each b-value was explored.

In the study of CIRs, we found that there was no statistical difference in the CIRs of hepatic lesions before and after enhancement on each of the b-value DW images.

© Annals of Translational Medicine. All rights reserved.

Table 2 CIRs of the focal hepatic lesions on DWI

Classification of lesions	b-value (s/mm^2)	Unenhanced	Enhanced	P value	Z value
HCC [47]	0	0.86±0.58	0.86±0.66	0.21	–1.264
	50	0.82±0.53	0.81±0.50	0.99	–0.017
	800	1.05±0.69	1.06±0.69	0.79	–0.271
	1,000	1.15±0.80	1.16±0.78	0.94	–0.07
	1,200	1.21±0.90	1.18±0.87	0.75	–0.317
Metastases [21]	0	0.97±0.52	0.93±0.56	0.74	–0.330
	50	0.81±0.58	0.94±0.58	0.39	–0.859
	800	1.2±0.98	1.02±0.73	0.47	–0.730
	1,000	1.24±0.87	1.41±0.90	0.07	–1.794
	1,200	1.32±1.05	1.56±1.00	0.10	–1.643
Cysts [12]	0	3.44±1.36	3.88±1.98	0.754	–0.314
	50	3.26±1.54	3.47±1.79	0.969	–0.039
	800	1.80±1.19	1.53±1.15	0.480	–0.706
	1,000	1.56±1.37	1.09±0.92	0.272	–1.099
	1,200	1.33±1.51	0.89±0.93	0.239	–1.177
Hemangiomas [12]	0	1.77±1.02	2.25±1.75	0.332	–0.971
	50	1.52±0.84	2.06±1.67	0.432	–0.787
	800	1.12±0.81	1.69±1.48	0.116	–1.573
	1,000	1.08±0.83	1.60±1.46	0.116	–1.571
	1,200	1.23±1.06	1.74±1.57	0.135	–1.494
Malignant lesions	0	0.90±0.56	0.88±0.57	0.741	–0.330
	50	0.82±0.54	0.86±0.54	0.664	–0.435
	800	1.10±0.78	1.04±0.70	0.470	–0.730
	1,000	1.18±0.81	1.23±0.83	0.159	–1.409
	1,200	1.24±0.94	1.32±0.93	0.100	–1.643
Benign lesions	0	2.60±1.45	3.06±2.01	0.355	–0.926
	50	2.39±1.50	2.76±1.84	0.637	–0.472
	800	1.46±1.06	1.61±1.30	0.475	–0.715
	1,000	1.32±1.13	1.35±1.22	0.742	–0.329
	1,200	1.28±1.22	1.31±1.33	0.775	–0.286
All lesions	0	1.34±1.15	1.45±1.48	0.664	–0.435
	50	1.23±1.13	1.35±1.34	0.982	–0.023
	800	1.19±0.87	1.19±0.94	0.946	–0.068
	1,000	1.21±0.90	1.32±1.05	0.294	–1.050
	1,200	1.25±1.03	1.45±1.48	0.165	–1.389

CIR, contrast intensity ratio; DWI, diffusion weighted imaging; HCC, hepatocellular carcinoma.

© Annals of Translational Medicine. All rights reserved.

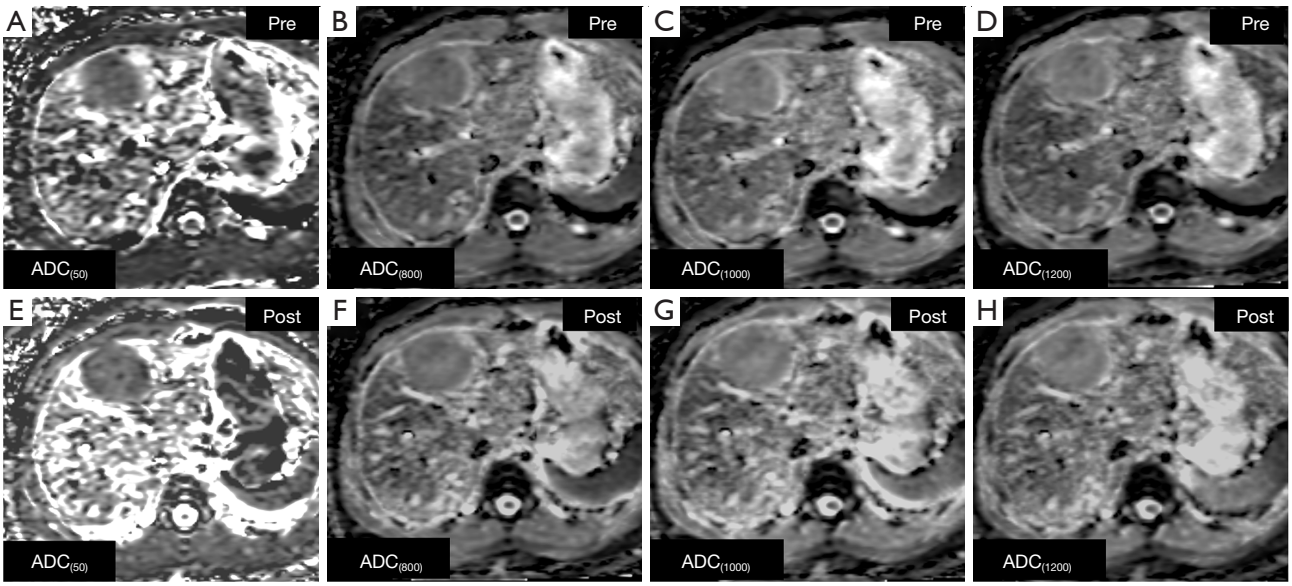

Figure 4 Male, 24 years old, HCC in right liver robe. (A-D) ADC map without Gd-EOB-DTPA; (E-H) ADC map with Gd-EOB-DTPA. (A,E) $ADC_{(50)}$; (B,F) $ADC_{(800)}$; (C,G) $ADC_{(1000)}$; (D,H) $ADC_{(1200)}$. The lesion displays in enhanced ADC were not different from unenhanced ADC. ADC, apparent diffusion coefficient; HCC, hepatocellular carcinoma.

A previous study conducted by Song *et al.* (11) also showed similar results, which proved that the enhanced DWI with Gd-EOB-DTPA would not result in a significant impact on the CIRs. However, the DWI sequence they used contained only one high b-value (800 s/mm^2), and thus, their conclusion was could not be applied different high b-value DWIs. In this study, we evaluated three high-b-value (800, 1,000, and 1,200 s/mm^2) images of the DWI sequence and found that there was no statistical differences in the pre- and post-contrast CIRs, further indicating that Gd-EOB-DTPA injection has no influence on the CIRs of high b-value DW images. Another study conducted by Muhi *et al.* (6) also compared the difference in CIRs before and after enhancement on two high b-values (500 and 1,000 s/mm^2), but their DWI sequences were acquired 20 minutes after Gd-EOB-DTPA injection, which was not the ideal delay time for enhanced DWI scans. According to Choi *et al.* (7), in order to optimize the process and reduce the scanning time, DWI scanning is recommended between the end of the dynamic enhanced image acquisition and the HBP. In our study, three phases of dynamic imaging (including arterial phase, portal phase, and equilibrium phase) were initially performed after the injection of Gd-EOB-DTPA, followed by T2 FSE images with a RT (usually 3–5 minutes). We then acquired the enhancement DW images at 10 minutes after injection, which maximally optimized the imaging process. In addition, Muhi *et al.* (6) only collected images of b-values =500 and 1,000 s/mm^2, lacking the evaluation of low b-values. DWI images with low b-values contain more information about blood perfusion (16), but have the limitation of reflecting the true diffusion. Our research found that there were no significant differences between the CIRs of low b-value images before and after enhancement. This finding differs slightly from the research of Choi *et al.* (7), which pointed out that the CNRs of HCC, malignant lesions, and all focal lesions were different before and after Gd-EOB-DTPA injection at the b-value =200 s/mm^2. This may be related to the different calculation methods; Choi *et al.* compared the CNR values, while we evaluated the CIR values.

Moreover, our results indicated that the ADC values of focal hepatic lesions were comparable on unenhanced and enhanced images at all b-values (P>0.05). This indicated that Gd-EOB-DTPA injection had no effect on the ADC values of focal hepatic lesions without uptake of contrast agents, which was similar to previous reports (6,7,11,17). Unlike previous reports that only discussed one single ADC value, this study evaluated the ADCs at four b-values (50, 800, 1,000, and 1,200 s/mm^2), and found no difference between the ADCs before and after enhancement, indicating that the ADC values of focal hepatic lesions

© Annals of Translational Medicine. All rights reserved.

Table 3 ADC values ($\times 10^{-3}$ mm^2/s) of the liver and focal hepatic lesions

Classification of lesions	ADCs	Unenhanced ($\times 10^{-3}$ mm^2/s)	Enhanced ($\times 10^{-3}$ mm^2/s)	P value	Z value
HCC	$ADC_{(50)}$	4.24±3.40	3.95±2.88	0.352	–0.931
	$ADC_{(800)}$	1.43±0.59	1.42±0.61	0.322	–0.990
	$ADC_{(1000)}$	1.29±0.44	1.26±0.41	0.533	–0.623
	$ADC_{(1200)}$	1.23±0.41	1.22±0.43	0.658	–0.443
Metastases	$ADC_{(50)}$	4.07±2.33	3.73±2.7	0.198	–1.286
	$ADC_{(800)}$	1.41±0.24	1.37±0.30	0.126	–1.530
	$ADC_{(1000)}$	1.19±0.23	1.17±0.26	0.305	–1.026
	$ADC_{(1200)}$	1.23±0.25	1.14±0.29	0.085	–1.721
Cysts	$ADC_{(50)}$	4.29±2.10	5.72±4.27	0.239	–1.177
	$ADC_{(800)}$	2.73±0.76	2.80±0.78	0.530	–0.628
	$ADC_{(1000)}$	2.68±0.74	2.64±0.71	0.209	–1.255
	$ADC_{(1200)}$	2.55±0.76	2.56±0.69	0.814	–0.236
Hemangiomas	$ADC_{(50)}$	2.81±1.13	2.71±1.13	0.099	–1.649
	$ADC_{(800)}$	2.27±1.33	2.07±0.55	0.239	–1.177
	$ADC_{(1000)}$	2.04±0.67	1.93±0.62	0.285	–1.069
	$ADC_{(1200)}$	1.91±0.84	1.86±0.63	0.504	–0.669
Malignant lesions	$ADC_{(50)}$	4.19±3.10	3.88±2.81	0.129	–1.518
	$ADC_{(800)}$	1.43±0.51	1.40±0.53	0.115	–1.577
	$ADC_{(1000)}$	1.26±0.39	1.23±0.37	0.278	–1.084
	$ADC_{(1200)}$	1.23±0.36	1.20±0.39	0.085	–1.724
Benign lesions	$ADC_{(50)}$	3.55±1.82	3.99±3.56	0.864	–0.171
	$ADC_{(800)}$	2.40±0.73	2.42±0.81	0.797	–0.257
	$ADC_{(1000)}$	2.30±0.77	2.27±0.85	0.088	–1.704
	$ADC_{(1200)}$	2.20±0.85	2.27±0.77	0.448	–0.758
All lesions	$ADC_{(50)}$	4.04±2.82	3.91±3.00	0.151	–1.431
	$ADC_{(800)}$	1.68±0.71	1.67±0.76	0.163	–1.394
	$ADC_{(1000)}$	1.53±0.69	1.50±0.70	0.078	–1.765
	$ADC_{(1200)}$	1.48±0.66	1.48±0.70	0.294	–1.049
Liver	$ADC_{(50)}$	8.61±10.21	7.86±2.88	0.005*	–2.784
	$ADC_{(800)}$	1.46±0.27	1.39±0.25	0.015*	–2.431
	$ADC_{(1000)}$	1.38±0.25	1.33±0.27	0.028*	–2.199
	$ADC_{(1200)}$	1.32±0.23	1.26±0.22	0.016*	–2.400

*, b=50 (NEX =1), 800 (NEX =4), 1,000 (NEX =4), 1,200 (NEX =4) s/mm^2. ADC, apparent diffusion coefficient; HCC, hepatocellular carcinoma; NEX, number of excitations.

© Annals of Translational Medicine. All rights reserved.

would not be affected by Gd-EOB-DTPA, regardless of whether this was a high b-value or low b-value DWI. However, unlike hepatic lesions, the post-contrast ADC values of normal hepatic parenchyma were significantly lower than those pre-contrast, which was speculated to be related to the uptake of Gd-EOB-DTPA by normal liver tissue (5-7).

By evaluating the diagnostic ability to distinguish benign from malignant lesions, we found that at high b-values (800, 1,000, and 1,200 s/mm^2), the ADC values of malignant tumors (HCCs and metastases) were lower than those of benign lesions (cysts and hemangiomas) in both pre- and post-contrast images (all P<0.001). This result was similar to the findings of Choi *et al.* (7), and showed that the DW images with a high b-value acquired 10 minutes after the injection of Gd-EOB-DTPA didn't affect the identification of benign and malignant hepatic lesions. However, previous studies (6,7,17) only analyzed one ADC value, which could not explain the fact that the enhanced ADCs at different b-value DWI images had the ability to discriminate between benign and malignant lesions. Besides high b-values, our study also analyzed the diagnostic ability of ADCs at low b-value (50 s/mm^2) DW images, and found it that this could not distinguish malignant from benign lesions. This was related to the principle in which the ADC maps obtained by low b-value DWIs reflected more blood perfusion information than water molecule movement (16).

In addition, this study also compared the diagnostic ability of ADCs at different b-values and found that the area under the ROC curve at b-values =800, 1,000, and 1,200 s/mm^2 were significantly larger than that at b=50 s/ mm^2. Also, among the high b-value DWI images, $ADC_{(1200)}$ had the largest area under the ROC curve, although it was not statistically different from $ADC_{(1000)}$ and $ADC_{(800)}$. This may be related to the principle in which the water molecular diffusion weight is heavier at higher b-value DWIs (18).

This study had several limitations that should be noted. Firstly, in this study, follow-up was used for the determination of benign lesions, as opposed to pathological analysis. Although the use of imaging follow-up is a common practice in academic liver imaging research (19), and is generally considered not to affect the determination of result, pathological analysis should still be used as the gold standard. Secondly, the sample size of this study is small. Lastly, none of the hepatic lesions involved in this study take up Gd-EOB-DTPA. Therefore, some other types of hepatic lesions, especially those ingesting Gd-EOB-DTPA, such as focal nodule hyperplasia (FNH), regenerative nodule (RN), etc. should be analyzed in the future studies.

In conclusion, our study demonstrated that DWI acquisition could be performed between dynamic enhanced scans and delayed hepatobiliary scans to save overall scanning time. The ADC values of the lesion were not affected by the injection of Gd-EOB-DTPA, regardless of the high or low b-values of DWI.

Acknowledgments

Funding: This study was supported by the Province Key Technology Research and Development Program of the Science & Technology Department of Sichuan Province (2020YFS0121, 2019YFS0434).

Footnote

Reporting Checklist: The authors have completed the STARD reporting checklist. Available at https://atm.amegroups.com/article/view/10.21037/atm-22-962/rc

Data Sharing Statement: Available at https://atm.amegroups.com/article/view/10.21037/atm-22-962/dss

Conflicts of Interest: All authors have completed the ICMJE uniform disclosure form (available at https://atm.amegroups.com/article/view/10.21037/atm-22-962/coif). LN and XW are from GE Healthcare China. The other authors have no conflicts of interest to declare.

Ethical Statement: The authors are accountable for all aspects of the work in ensuring that questions related to the accuracy or integrity of any part of the work are appropriately investigated and resolved. The study was conducted in accordance with the Declaration of Helsinki (as revised in 2013). This diagnostic and observational study was approved by the institutional review board of biomedical ethics branch of West China Hospital, Sichuan University [No. 2016(297)], and written informed consent was obtained from all patients.

Open Access Statement: This is an Open Access article distributed in accordance with the Creative Commons Attribution-NonCommercial-NoDerivs 4.0 International License (CC BY-NC-ND 4.0), which permits the non-commercial replication and distribution of the article with the strict proviso that no changes or edits are made and the

© Annals of Translational Medicine. All rights reserved.

original work is properly cited (including links to both the formal publication through the relevant DOI and the license). See: https://creativecommons.org/licenses/by-nc-nd/4.0/.

References

1. Alanazi SA, Alanazi F, Haq N, et al. Lipoproteins-Nanocarriers as a Promising Approach for Targeting Liver Cancer: Present Status and Application Prospects. Curr Drug Deliv 2020;17:826-44.
2. Torre LA, Bray F, Siegel RL, et al. Global cancer statistics, 2012. CA Cancer J Clin 2015;65:87-108.
3. Tsai WC, Kung PT, Wang YH, et al. Influence of the time interval from diagnosis to treatment on survival for early-stage liver cancer. PLoS One 2018;13:e0199532.
4. Sofue K, Tsurusaki M, Tokue H, et al. Gd-EOB-DTPA-enhanced 3.0 T MR imaging: quantitative and qualitative comparison of hepatocyte-phase images obtained 10 min and 20 min after injection for the detection of liver metastases from colorectal carcinoma. Eur Radiol 2011;21:2336-43.
5. Cieszanowski A, Podgórska J, Rosiak G, et al. Gd-EOB-DTPA-Enhanced MR Imaging of the Liver: The Effect on T2 Relaxation Times and Apparent Diffusion Coefficient (ADC). Pol J Radiol 2016;81:103-9.
6. Muhi A, Ichikawa T, Motosugi U, et al. Diffusion- and T_2-weighted MR imaging of the liver: effect of intravenous administration of gadoxetic acid disodium. Magn Reson Med Sci 2012;11:185-91.
7. Choi JS, Kim MJ, Choi JY, et al. Diffusion-weighted MR imaging of liver on 3.0-Tesla system: effect of intravenous administration of gadoxetic acid disodium. Eur Radiol 2010;20:1052-60.
8. Park YS, Lee CH, Kim JH, et al. Effect of Gd-EOB-DTPA on hepatic fat quantification using high-speed T2-corrected multi-echo acquisition in (1)H MR spectroscopy. Magn Reson Imaging 2014;32:886-90.
9. Saito K, Yoshimura N, Shirota N, et al. Distinguishing liver haemangiomas from metastatic tumours using gadolinium ethoxybenzyl diethylenetriamine pentaacetic acid-enhanced diffusion-weighted imaging at 1.5T MRI. J Med Imaging Radiat Oncol 2016;60:599-606.
10. Taouli B. Diffusion-weighted MR imaging for liver lesion characterization: a critical look. Radiology 2012;262:378-80.
11. Song KD, Kim YK, Lee WJ, et al. Detection and characterization of small focal hepatic lesions (≤2.5 cm in diameter): a comparison of diffusion-weighted images before and after administration of gadoxetic acid disodium at 3.0T. Acta Radiol 2012;53:485-93.
12. Parikh T, Drew SJ, Lee VS, et al. Focal liver lesion detection and characterization with diffusion-weighted MR imaging: comparison with standard breath-hold T2-weighted imaging. Radiology 2008;246:812-22.
13. van den Bos IC, Hussain SM, Krestin GP, et al. Liver imaging at 3.0 T: diffusion-induced black-blood echo-planar imaging with large anatomic volumetric coverage as an alternative for specific absorption rate-intensive echo-train spin-echo sequences: feasibility study. Radiology 2008;248:264-71.
14. Taouli B, Vilgrain V, Dumont E, et al. Evaluation of liver diffusion isotropy and characterization of focal hepatic lesions with two single-shot echo-planar MR imaging sequences: prospective study in 66 patients. Radiology 2003;226:71-8.
15. Taouli B, Koh DM. Diffusion-weighted MR imaging of the liver. Radiology 2010;254:47-66.
16. Yamada I, Aung W, Himeno Y, et al. Diffusion coefficients in abdominal organs and hepatic lesions: evaluation with intravoxel incoherent motion echo-planar MR imaging. Radiology 1999;210:617-23.
17. Benndorf M, Schelhorn J, Dietzel M, et al. Diffusion weighted imaging of liver lesions suspect for metastases: Apparent diffusion coefficient (ADC) values and lesion contrast are independent from Gd-EOB-DTPA administration. Eur J Radiol 2012;81:e849-53.
18. Bammer R. Basic principles of diffusion-weighted imaging. Eur J Radiol 2003;45:169-84.
19. Löwenthal D, Zeile M, Lim WY, et al. Detection and characterisation of focal liver lesions in colorectal carcinoma patients: comparison of diffusion-weighted and Gd-EOB-DTPA enhanced MR imaging. Eur Radiol 2011;21:832-40.

(English Language Editor: A. Kassem)

Cite this article as: Tang H, Yuan Y, Deng L, Wei Y, Chen G, Zhang T, Nie L, Wei X, Song B, Li Z. Identification of diffusion weighted imaging would be affected before and after Gd-EOB-DTPA in patients with focal hepatic lesions: an observational study. Ann Transl Med 2022;10(6):346. doi: 10.21037/atm-22-962

© Annals of Translational Medicine. All rights reserved.